Carbohydrate Polymers 83 (2011) 973–978

Contents lists available at ScienceDirect

Carbohydrate Polymers

journal homepage: www.elsevier.com/locate/carbpol

Fabrication of polymer/layered silicate intercalated nanofibrous mats and their bacterial inhibition activity

Hongbing Deng[a,b,1], Xueyong Li[c,1], Bin Ding[b,d,*], Yumin Du[a,**], Guoxiang Li[a], Jianhong Yang[a], Xianwen Hu[a]

[a] School of Resource and Environmental Science, Wuhan University, Wuhan 430079, China
[b] State Key Laboratory for Modification of Chemical Fibers and Polymer Materials, College of Materials Science and Engineering, Donghua University, Shanghai 201620, China
[c] Department of Plastic Surgery, Tangdu Hospital, Fourth Military Medical University, Xi'an, 710038, China
[d] Nanomaterials Research Center, Modern Textile Institute, Donghua University, Shanghai 200051, China

ARTICLE INFO

Article history:
Received 4 August 2010
Received in revised form 24 August 2010
Accepted 5 September 2010
Available online 21 September 2010

Keywords:
Electrospinning
Chitosan
Layered silicate
Poly(vinyl alcohol)
Bacterial inhibition activity

ABSTRACT

A uniform electrospun nanofibrous membrane was fabricated from chitosan (CS)–polyvinyl alcohol (PVA)/organic rectorite (OREC) with different mixing ratios by solution-mixing process and eleltrospinning technologies. The morphology, intercalation between polymer and OREC, and bacterial inhibition activity of the electrospun membranes were investigated. Field emission scanning electron microscopy showed uniform fibrous structure generated with the addition of OREC. Energy-dispersive X-ray spectroscopy results confirmed the existence of OREC on the surface of electrospun membranes. Fourier transform infrared spectra and small angle X-ray diffraction results verified that the interlayer of OREC was intercalated by CS and PVA chains successfully. The controllable interlayer distance of OREC was enlarged from 3.68 to 4.28 nm. The membranes had enhanced bacterial inhibition activity with the addition of OREC.

1. Introduction

Polymer/layered silicate composite nanofibers have unique physical and chemical properties of both inorganic and organic materials (Wang et al., 2006). They also have characteristics of nanofibers such as ultrafine diameter, high surface area-to-volume ratio, three-dimensional (3D) nanofibrous structure, etc. (Ding, Kimura, Sato, Fujita, & Shiratori, 2004; Ding, Li, Miyauchi, Kuwaki, & Shiratori, 2006; Ji et al., 2006; Lee, Kim, Chen, Shao-Horn, & Hammond, 2009; Yang, Tao, Pang, & Siu, 2008). Recently, polymer/layered silicate nanofibers and their potential applications in aerospace, biodegradable materials, catalysis, etc. have been studied (Njuguna & Pielichowski, 2004; Wypych & Satyanarayana, 2005; Marras, Kladi, Tsivintzelis, Zuburtikudis, & Panayiotou, 2008; Su, 2009). In our group, we have previously found a type of preferred rectorite (REC), especially organic rectorite (OREC) modified from REC (Wang, Du, Luo, Lin, & Kennedy, 2007; Wang, Pei, Du, & Li, 2008; Wang, Du, Luo, et al., 2009; Wang, Du, Sun, & Liu, 2009). It has larger interlayer distance, better separable layer thickness and layer aspect ratio than regular montmorillonite (MMT), which may have more favorable properties that could be used in relative applications (Wang et al., 2007; Wang, Pei, et al., 2008; Wang, Du, Luo, et al., 2009; Wang, Du, Sun, et al., 2009). Although several polymer/layered silicate nanocomposite products with different shapes and applications are now available, only a few nanofibrous membranes are studied based on polymer/MMT (Wang et al., 2006, 2007).

Electrospinning has been considered as an efficient and simple method to fabricate submicron-sized fibers, which involves generation of a jet of viscous solution and formation of ultra-fine fibers (Sakai, Antoku, Yamaguchi, & Kawakami, 2008; Yu et al., 2009). In order to fabricate electrospun polymer/layered silicate nanofibrous membranes, polymers were mixed with OREC. Chitosan (CS) is a polysaccharide that has a number of properties such as haemostatic activity (Bonferoni, Sandri, Rossi, Ferrari, & Caramella, 2009; Spasova, Paneva, Manolova, Radenkov, & Rashkov, 2008), non-toxicity (Neamnark et al., 2007; Wu, Wei, Wang, Su, & Ma, 2007; Zhu, Chen, Yuan, Wu, & Lu, 2006), biodegradability (Bagheri-Khoulenjani, Taghizadeh, & Mirzadeh, 2009; Li, Leung, Hopper, Ellenbogen, & Zhang, 2010), and intrinsic antibacterial properties (Sajomsang, Tantayanon, Tangpasuthadol, & Daly, 2009; Sanpo,

* Corresponding author at: State Key Laboratory for Modification of Chemical Fibers and Polymer Materials, College of Materials Science and Engineering, Donghua University, Shanghai 201620, China. Tel.: +86 21 62378202; fax: +86 21 62378392.
** Corresponding author. Tel.: +86 27 68778501; fax: +86 27 68778501.
E-mail addresses: binding@dhu.edu.cn (B. Ding), duyumin@whu.edu.cn (Y. Du).
[1] Both the authors contributed equally to this work.

0144-8617/$ – see front matter © 2010 Elsevier Ltd. All rights reserved.
doi:10.1016/j.carbpol.2010.09.008

Ang, Cheang, & Khor, 2009). Therefore, it is preferred to be used in antibacterial applications. However, there are only a few reports on CS/layered silicate nanocomposites based on MMT (Liu, Liu, Chen, & Liu, 2008; Podsiadlo, Tang, & Kotov, 2005; Wang, Du, & Luo, 2008). Darder, Colilla, and Ruiz-Hitzky (2003) and Darder, Colilla, and Ruiz-Hitzky (2005) have synthesized functional CS/MMT nanocomposites, which have been successfully used in the development of bulk modified electrodes. In their study, the prepared CS/MMT nanocomposites based on only pristine MMT but not modified MMT. Consequently, the obtained interlayer distance was not very large, which may directly affect the improvement of the material properties. On the other hand, a few people studied CS/layered silicate nanofibers with addition of REC. Wang et al. (2006) and Wang, Du, Sun, et al. (2009) have examined the antibacterial activity of CS/OREC and quaternized chitosan/OREC nanocomposite, and revealed that OREC could enhance the degree of bacterial inhibition. However, the formation of nanofibers based on chitosan–rectorite intercalated has not yet been studied.

In the past decade, several research groups have tried to generate uniform nanofiber from pure CS, but it was proved to be difficult because of its viscosity, conductivity and surface tension (De Vrieze, Westbroek, Van Camp, & Van Langenhove, 2007; Geng, Kwon, & Jang, 2005; Ohkawa, Cha, Kim, Nishida, & Yamamoto, 2004). Therefore, polymers that could generate fibers easily such as poly(vinyl alcohol) (PVA) were added to assist fiber formation. Recently, more and more researchers have investigated the morphology of nanofibers fabricated from CS (or derivatives of CS)/PVA mixture (Sajeev, Anand, Menon, & Nair, 2008; Zhang et al., 2007; Zhou, Yang, & Nie, 2007). It was found that the properties of polymers, including concentration, blending ratio and some process parameters, will affect the fiber morphology.

In this study, OREC was prepared by cation exchange from REC. Then a series of CS–OREC intercalated composite based nanofibrous membranes was fabricated. The morphology of the nanofibers and effect of OREC on the antibacterial activity of these electrospun nanofibrous membranes were examined.

2. Experimental

Chitosan (CS, $M_w = 2.0 \times 10^5$ kDa) from shrimp shell with 92% deacetylation was from Zhejiang Yuhuan Ocean Biochemical Co., China. Calcium rectorite (Ca^{2+}-REC) refined from the clay minerals was provided by Hubei Mingliu Inc. Co., China. PVA ($M_w = 9 \times 10^4$) was purchased from Wako Pure Chemical Industries, Japan. Acetic acid was purchased from Aladdin Chemical Reagent Co., China. All aqueous solutions were prepared using purified water with a resistance of 18.2 MΩ cm.

2% CS solution was prepared by adding CS into 2% acetic acid with constant agitation in close vials for 2 h at room temperature. 7% PVA solution was prepared by dissolving PVA in distilled water at 70 °C with gentle magnetic stirring for 4 h. OREC was prepared by sodium dodecylsulfonate cation exchange reactions as was described previously (Wang et al., 2006, 2007). The OREC suspension was pretreated by ultrasonication. Then 2% chitosan solution was added dropwise and slowly into OREC suspensions at 60 °C under gentle agitation for 12 h to obtain mixed solutions. The resultant homogeneous solutions with the aqueous PVA solution were mixed to obtain CS/PVA mixture at 10/90, 20/80, 30/70, 40/60, 50/50 and 60/40 mass ratios. All the CS/PVA mixture solutions used for electrospinning contain 1% OREC. The concentrations of all solutions were expressed in wt/wt%.

The electrospinning solution was fed into a plastic syringe driven by a syringe pump (LSP02-1B, Baoding Longer Precision Pump Co., Ltd., China). The positive electrode of a high voltage power supply (DW-P303-1ACD8, Tianjin Dongwen Co., China) was clamped to the metal needle tip of the syringe, and the cylindrical collector covered by aluminum foil was grounded. The applied voltage was 17 kV, and the tip-to-collector distance was 15 cm. The ambient temperature and relative humidity were maintained at 25 °C and 45%, respectively. The prepared fibrous membranes were dried in vacuum at room temperature to remove the trace solvent.

Table 1
ζ-Potential (mV) of OREC powder, CS powder, and CS–OREC composite particles (12/1).

Samples	OREC	CS	CS–OREC
ζ-Potential (mV)	−8.3	25.1	27.6

Field emission scanning electron microscopy (FE-SEM) and energy-dispersive X-ray (EDX) spectroscopy images were obtained by Hitachi S-4800 (S-4800, Hitachi Ltd., Japan). Fourier transform infrared (FT-IR) spectra were recorded by Nicolet170-SX (Thermo Nicolet Ltd., USA). The small angle X-ray diffraction (SAXRD) was performed on type D/max-rA diffractometer (Rigaku Co., Japan) with Cu target and Kα radiation (λ = 0.154 nm). Optical density (OD) in the bacteria inhibition experiment was determined by ultraviolet (UV)–visible spectrometer UV–vis (722 s, Shanghai Precision & Scientific Instrument Co., Ltd., China). ζ-Potential analysis was preformed using a Nano-25 zetasizer (Malven, England).

The antibacterial activity of nanofibrous membranes was measured according to previous study (25). Gram-negative *Escherichia coli* was selected as a representative bacterial and cultivated in culture medium in an incubator. The nanofibrous mats were sterilized under an ultraviolet radiation lamp for 30 min, cut in squares of 1×1 cm^2, and incubated with 10^7 CFU/mL *E. coli* in bacterial culture medium at 37 °C for 18 h. Based on the optical density (OD) from the UV–vis measurement, the antibacterial activity was calculated using the following equation:

$$\text{Antibacterial activity} = \frac{A - B}{A} \times 100\% \quad (1)$$

where A and B are the OD of surviving cells in control and test samples, respectively.

3. Results and discussion

Fig. 1 shows the typical FE-SEM images of fibrous membranes electrospun from CS/PVA/OREC mixture solutions with 1% OREC and different CS/PVA weight ratios. The microstructure of composite nanofibers was affected by the variation of the mixture compositions. The diameters of fibers fabricated from pure PVA (Fig. 1a) were much thicker than that of the fibers fabricated from the solutions containing CS, because CS can form ultra-fine nanofibers and the fiber generating efficiency was much less than that of PVA. In addition, beads can be observed in the nanofibrous mats and the average diameter of spun-nanofibers decreased when CS content increased in the mixed solution, which was caused by different viscosity and conductivity of CS and PVA solution. CS is a weak natural cationic polysaccharide because its amino group is easily protonated in aqueous media, especially at low pH. Oppositely, PVA solution tends to be neutral and the OREC will become anionic in this solution (Table 1). These results suggested that the different properties of the three components in the mixture solution could affect the properties of the blend solution and the formation of fibers.

As we know, the main components of OREC are Si, Al, and Na elements. EDX spectrum was next recorded to identify the existence of the compositions of OREC from a selected rectangle area of CS–OREC/PVA composite nanofibrous mats. As is shown in Fig. 2a, the characteristic peaks of Si, Al, and Na elements were detected in the spectrum. The EDX data confirmed that OREC existed in

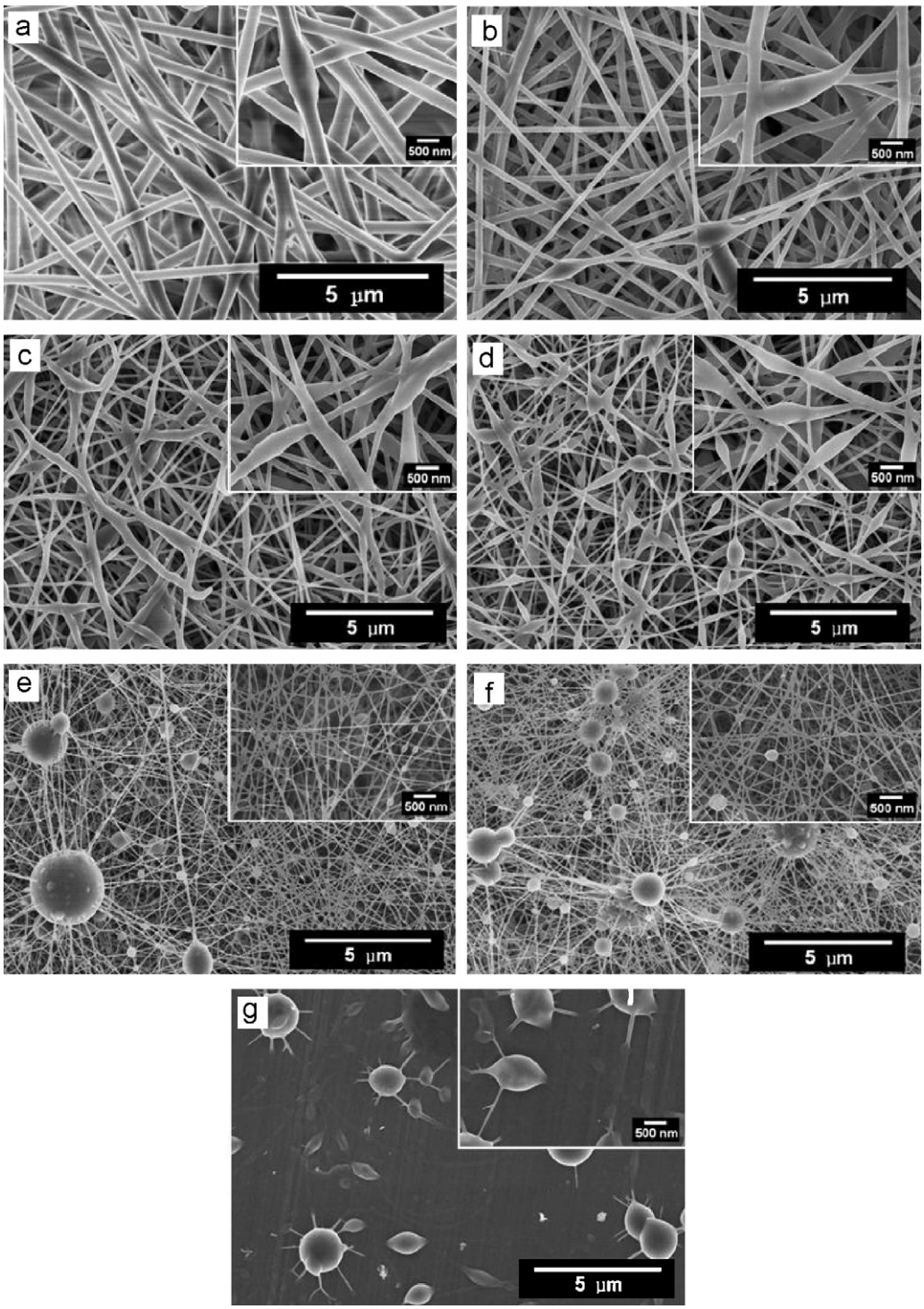

Fig. 1. FE-SEM images of nanofibrous membranes electrospun from solutions with various CS/PVA mass ratios containing 1% OREC: (a) 0/100, (b) 10/90, (c) 20/80, (d) 30/70, (e) 40/60, (f) 50/50 and (g) 60/40.

the nanofibrous mats. Fig. 2b shows that the throughput ratio of nanofibers and the number of beads were correlated with CS/PVA mass ratios. The diameters and the throughput ratio were proportional to PVA content. These results were consistent with previous studies (Sajeev et al., 2008; Zhang et al., 2007; Zhou et al., 2007).

In order to investigate the effect of OREC on electrospun fiber formation, various concentrations of OREC in the mixture was regulated at 0.1%, 1%, 1.5%, 2% and 3%, (Figs. 1c and 3). All the nanofibrous mats maintained good fiber shape with the introduction of different concentrations of OREC. When the concentrations of OREC were higher than 1%, there were blocks reunited in the as-spun fibers, which were undesirable for electrospun nanofibers. When the concentration of OREC was as low as 0.1%, there was no visible difference in the morphology of fiber mats, compared with the morphology of fiber mats when the OREC concentration was 1%.

Fig. 4a and b showed the morphology of the electrospun CS/PVA composite nanofibers at CS/PVA mass ratios of 30/60 and 40/70. Compared with the nanofibers at CS/PVA mass ratios of 30/60 (Fig. 1d) and 40/70 (Fig. 1e) that have OREC, the nanofibrous mats fabricated from only CS/PVA without OREC formed more beads

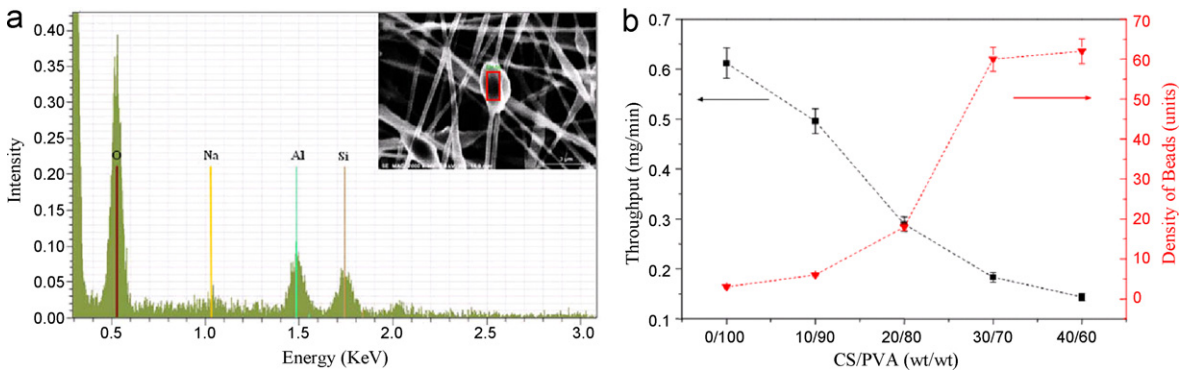

Fig. 2. (a) EDX spectrum of selected composite nanofibrous membranes electrospun from solutions containing 1 wt% OREC with CS/PVA weight ratio of 40/60 and (b) throughput and the density of beads per unit area of fibrous membranes produced with various CS/PVA mass ratios.

and had much smaller diameters (Fig. 4a and b). It is known that when the conductivity of the electrospinning solution increases, the beads formation is decreased. The electrical charge of OREC increased solution conductivity, therefore, beads formation was decreased when nanoclay was added. Moreover, nanofibers in Fig. 4a displayed fewer beads and thicker diameters than that in Fig. 4b, because the concentration of CS was higher in Fig. 4a. In summary, when OREC was added, the diameter of as-spun nanofibers and the number of beads will decrease remarkably.

Fig. 5 shows the FT-IR spectra of all the electrospun composite nanofibers and the raw materials. CS has resonance bands at 3423 and 1654 cm^{-1}, commonly known as the N–H stretching of the primary amino groups and the carbonyl stretching of the secondary amide band (Lim & Hudson, 2004). PVA nanofibrous mats showed absorption bands at 3383, 2941, 1734, 1098, and 850 cm^{-1}, characteristic of the O–H, $-CH_2$, C=O, C–O, and C–C resonances, respectively (Li & Hsieh, 2006). OREC exhibited dominant peaks at 467 and 546 cm^{-1}, which was assigned to Si–O bending vibration, 910 and 3643 cm^{-1} bands mean –OH vibration, 1025 and 1050 cm^{-1} stand for Si–O stretching vibration band, and 1650 cm^{-1} causes by the bending vibration of H_2O (Wang et al., 2006; Wang, Du, Sun, et al., 2009). The OREC was synthesized from REC before preparing the stock solution for electrospinning. There was little change in the frequency and relative intensity of the peaks of OREC and REC. Only the peaks appearing at 2921 cm^{-1} and 2851 cm^{-1} showed some differences, which was attributed to the $-CH_2$, $-CH_3$ stretching vibrations (Wang et al., 2006). This result indicated that sodium dodecylsulfonate has been successfully exchanged into the interlayer of unmodified Ca^{2+}-REC.

In the spectra of PVA/OREC and CS/PVA/OREC nanofibrous mats, the band of OREC at 3643 cm^{-1} disappeared, which implied that the –OH of OREC reacted with PVA or CS. The –OH of OREC may form ether bond with the –OH of CS or PVA, and possibly generate hydrogen bond with the amino group of CS. Compared with CS,

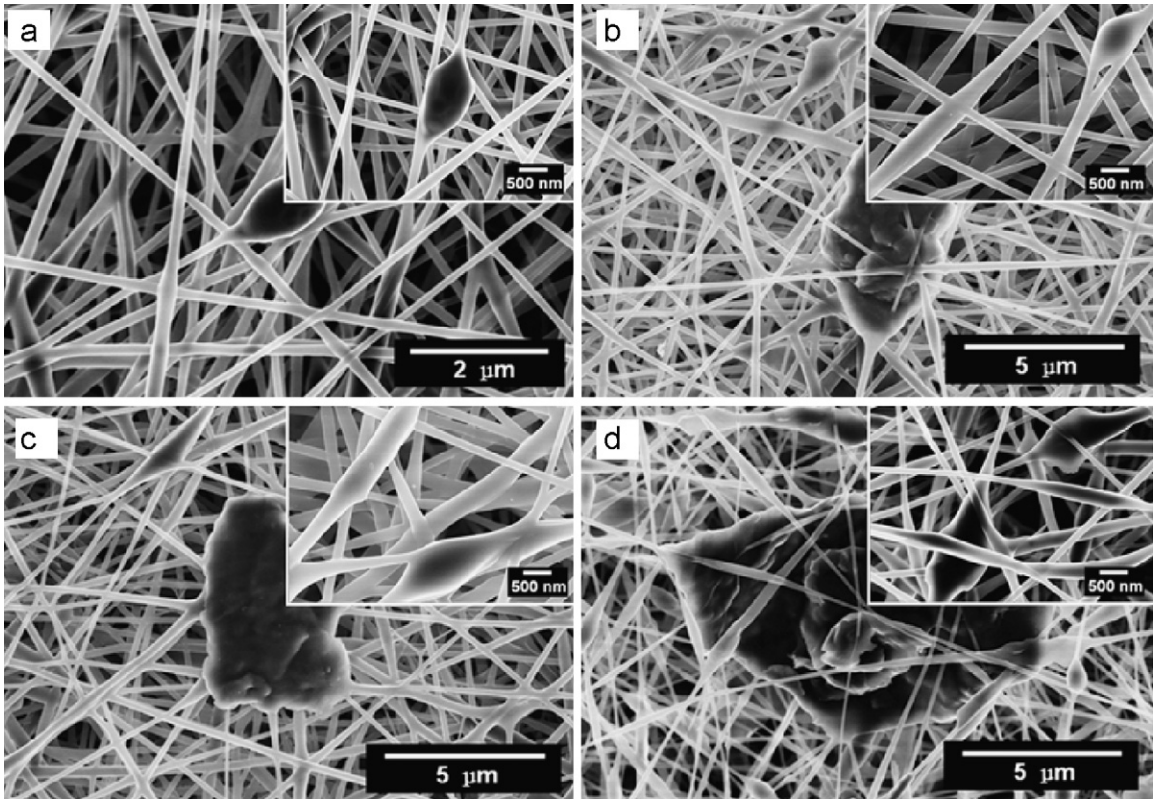

Fig. 3. FE-SEM images of nanofibrous membranes fabricated from CS/PVA (20/80) mixture containing various content of OREC: (a) 0.1 wt%, (b) 1.5 wt%, (c) 2 wt%, and (d) 3 wt%.

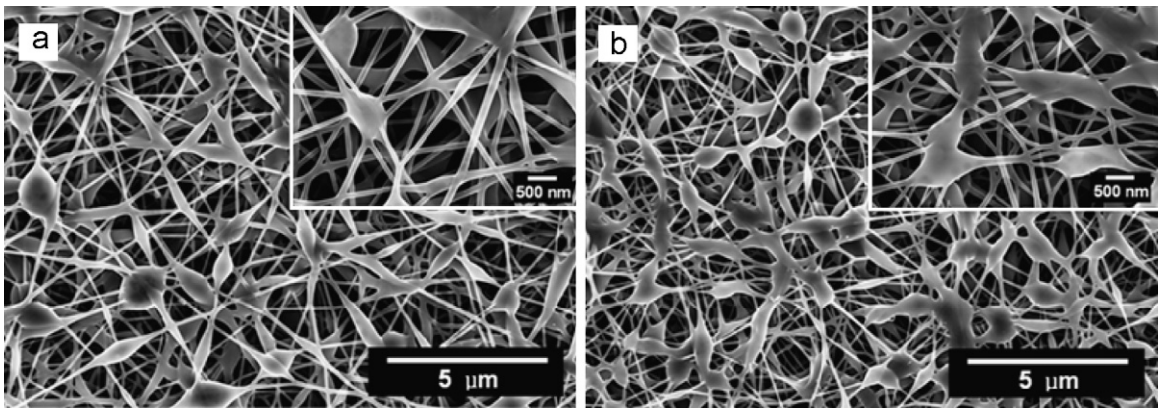

Fig. 4. FE-SEM images of nanofibrous membranes electrospun from CS/PVA mixture without OREC: (a) 30/70 and (b) 40/60.

CS/PVA and PVA/OREC, the peak around 3448 cm^{-1} became wider and stronger in the CS/PVA/OREC composite nanofibrous mats. Moreover, the N–H bonded to O–H vibration band at 3448 cm^{-1} in CS shifts towards lower frequency no matter what it blends with. It revealed that the $-NH_2$ and –OH groups of CS formed hydrogen bonds with the –OH group of OREC and PVA. A strong hydrogen bonding interaction may also form between and inside CS molecules when they are constrained in the gallery of OREC layers, as is seen in the spectra of the CS /PVA/OREC nanofibers with the largest loading of CS chains into the interlayer of OREC, where the N–H and O–H vibrations shift to the lowest frequency (3419 cm^{-1}).

To investigate the building of pre-designed intercalated architecture in composite nanofibrous mats, the SAXRD patterns of fibrous samples were recorded to measure the change of gallery distance of OREC before and after intercalation (Fig. 6). The distance between OREC is 3.68 nm, which is calculated by the Bragg's equation (2):

$$2d \sin\theta = n\lambda. \quad (2)$$

where d is the interlayer spacing, θ is the angle of incidence, λ is wave length and n is an integer, standing for the order of the reflection. The SAXRD curves of the OREC based nanofibers diminished in comparison with the curve of OREC. CS resulted in a much bigger distance enhancement than PVA, because the cationic amido of CS which was intercalated into the interlayer of OREC generated electrostatic repulsion force and compelled the distance of the interlayer to become large enough to accomplish a harmonious balance. As shown in the FT-IR spectra, the hydrogen bond between CS and OREC is another reason for intercalation. For PVA chains there were merely general infiltration and hydrogen bonds. CS is more efficient than PVA in the intercalation process.

The degree of bacteria growth inhibition of *E. coli* was examined with the composition of as-spun nanofibrous mats. It was found that all CS based nanofibrous mats exhibited antibacterial activ-

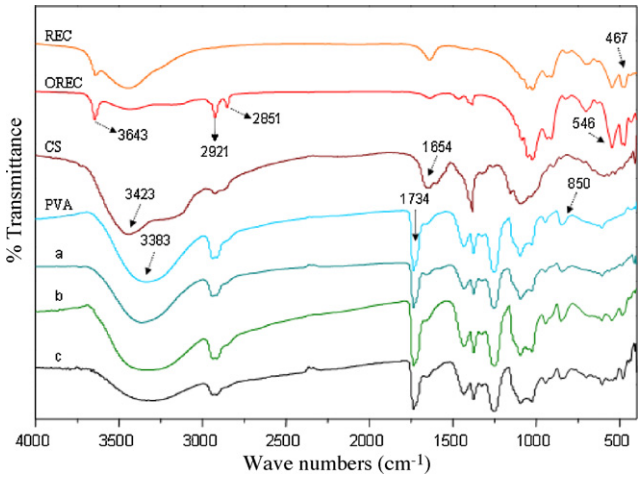

Fig. 5. FT-IR spectra of REC powder, OREC powder, CS powder, PVA fibers and their composite fibrous membranes: (a) CS/PVA, (b) PVA/OREC and (c) CS/PVA/OREC composite fibrous membrane with CS/PVA weight ratio of 40/60.

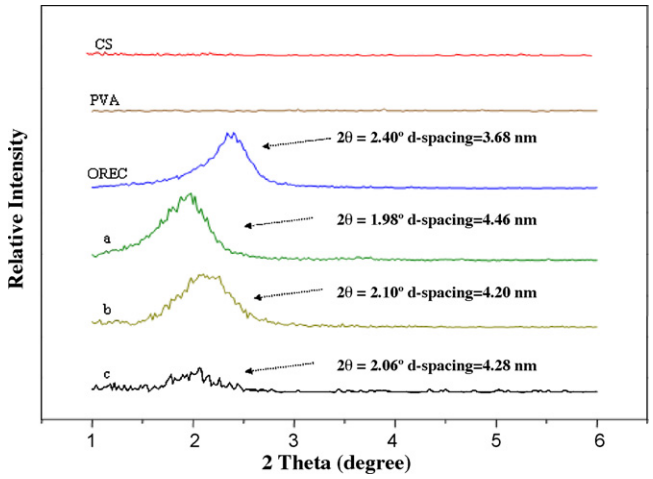

Fig. 6. SAXRD patterns of CS powder, PVA fibers, OREC powder and their composite fibrous membranes containing 1 wt% OREC: (a) CS/OREC, (b) PVA/OREC and (c) CS/PVA/OREC composite fibrous membrane with CS/PVA weight ratio of 40/60.

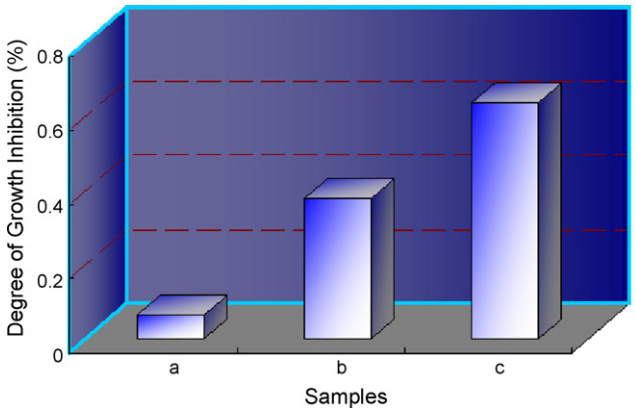

Fig. 7. Degree of bacterial growth inhibition of electrospun fibrous mats: (a) PVA, (b) CS/PVA = 40/60, and (c) CS/PVA = 40/60 containing 1 wt% OREC.

ity (Fig. 7). The CS–OREC/PVA nanofibrous mats exhibited a degree of growth inhibition of 60%, the CS/PVA mats showed a degree of growth inhibition below 40%, and the PVA nanofibrous mats showed little antibacterial activity. These results indicated that the degree of growth inhibition of the as-spun mats with the introduction of OREC was the highest, which revealed that the addition of OREC improved the antibacterial ability of the nanofibrous mats. The enhancement of the degree of growth inhibition with the addition of OREC was consistent with the previous report (Wang et al., 2006). The results also suggested that CS has better antimicrobial activity than PVA.

4. Conclusions

In this study, CS–OREC based nanofibrous cellulose mats with antibacterial property were successfully prepared via electrospinning. The morphology of the as-spun nanofibrous mats was greatly influenced by the composition of the solutions including CS/PVA weight ratios and the amount of OREC. The resultant samples maintained good fiber shape and 3D structure. The FT-IR and EDX results demonstrated that OREC existed in the fibers. The SAXRD data showed that OREC was intercalated by CS and the interlayer distance between OREC was enlarged by CS chains. The introduction of OREC in nanofibrous mats led to better antibacterial activity.

Acknowledgments

This project was funded by the State Key Laboratory for Modification of Chemical Fibers and Polymer Materials, Donghua University, China. Partial support from the Program of Introducing Talents of Discipline to Universities (No. 111-2-04 and B07024).

References

Bagheri-Khoulenjani, S., Taghizadeh, S. M., & Mirzadeh, H. (2009). An investigation on the short-term biodegradability of chitosan with various molecular weights and degrees of deacetylation. *Carbohydrate Polymers*, *78*, 773–778.

Bonferoni, M. C., Sandri, G., Rossi, S., Ferrari, F., & Caramella, C. (2009). Chitosan and its salts for mucosal and transmucosal delivery. *Expert Opinion on Drug Delivery*, *6*, 923–939.

Darder, M., Colilla, M., & Ruiz-Hitzky, E. (2003). Biopolymer–clay nanocomposites based on chitosan intercalated in montmorillonite. *Chemistry of Materials*, *15*, 3774–3780.

Darder, M., Colilla, M., & Ruiz-Hitzky, E. (2005). Chitosan–clay nanocomposites: Application as electrochemical sensors. *Applied Clay Science*, *28*, 199–208.

De Vrieze, S., Westbroek, P., Van Camp, T., & Van Langenhove, L. (2007). Electrospinning of chitosan nanofibrous structures: Feasibility study. *Journal of Materials Science*, *42*, 8029–8034.

Ding, B., Kimura, E., Sato, T., Fujita, S., & Shiratori, S. (2004). Fabrication of blend biodegradable nanofibrous nonwoven mats via multi-jet electrospinning. *Polymer*, *45*, 1895–1902.

Ding, B., Li, C. R., Miyauchi, Y., Kuwaki, O., & Shiratori, S. (2006). Formation of novel 2D polymer nanowebs via electrospinning. *Nanotechnology*, *17*, 3685–3691.

Geng, X. Y., Kwon, O. H., & Jang, J. H. (2005). Electrospinning of chitosan dissolved in concentrated acetic acid solution. *Biomaterials*, *26*, 5427–5432.

Ji, Y., Ghosh, K., Shu, X. Z., Li, B. Q., Sokolov, J. C., Prestwich, G. D., et al. (2006). Electrospun three-dimensional hyaluronic acid nanofibrous scaffolds. *Biomaterials*, *27*, 3782–3792.

Lee, S. W., Kim, B. S., Chen, S., Shao-Horn, Y., & Hammond, P. T. (2009). Layer-by-layer assembly of all carbon nanotube ultrathin films for electrochemical applications. *Journal of the American Chemical Society*, *131*, 671–679.

Li, L., & Hsieh, Y. L. (2006). Chitosan bicomponent nanofibers and nanoporous fibers. *Carbohydrate Research*, *341*, 374–381.

Li, Z. S., Leung, M., Hopper, R., Ellenbogen, R., & Zhang, M. Q. (2010). Feeder-free self-renewal of human embryonic stem cells in 3D porous natural polymer scaffolds. *Biomaterials*, *31*, 404–412.

Lim, S. H., & Hudson, S. M. (2004). Synthesis and antimicrobial activity of a water-soluble chitosan derivative with a fiber-reactive group. *Carbohydrate Research*, *339*, 313–319.

Liu, K. H., Liu, T. Y., Chen, S. Y., & Liu, D. M. (2008). Drug release behavior of chitosan-montmorillonite nanocomposite hydrogels following electro stimulation. *Acta Biomaterialia*, *4*, 1038–1045.

Marras, S. I., Kladi, K. P., Tsivintzelis, L., Zuburtikudis, I., & Panayiotou, C. (2008). Biodegradable polymer nanocomposites: The role of nanoclays on the thermomechanical characteristics and the electrospun fibrous structure. *Acta Biomaterialia*, *4*, 756–765.

Neamnark, A., Sanchavanakit, N., Pavasant, P., Bunaprasert, T., Supaphol, P., & Rujiravanit, R. (2007). In vitro biocompatibility evaluations of hexanoyl chitosan film. *Carbohydrate Polymers*, *68*, 166–172.

Njuguna, J., & Pielichowski, K. (2004). Polymer nanocomposites for aerospace applications: Fabrication. *Advanced Engineering Materials*, *6*, 193–203.

Ohkawa, K., Cha, D. I., Kim, H., Nishida, A., & Yamamoto, H. (2004). Electrospinning of chitosan. *Macromolecular Rapid Communications*, *25*, 1600–1605.

Podsiadlo, P., Tang, Z. Y., & Kotov, N. A. (2005). Layer-by-layer assembly of Na^+-montmorillonite/chitosan thin films: Chitosan-based "artificial Nacre". *Abstracts of Papers of the American Chemical Society*, *229*, U734.

Sajeev, U. S., Anand, K. A., Menon, D., & Nair, S. (2008). Control of nanostructures in PVA, PVA/chitosan blends and PCL through electrospinning. *Bulletin of Materials Science*, *31*, 343–351.

Sajomsang, W., Tantayanon, S., Tangpasuthadol, V., & Daly, W. H. (2009). Quaternization of N-aryl chitosan derivatives: Synthesis, characterization, and antibacterial activity. *Carbohydrate Research*, *344*, 2502–2511.

Sakai, S., Antoku, K., Yamaguchi, T., & Kawakami, K. (2008). Transesterification by lipase entrapped in electrospun poly(vinyl alcohol) fibers and its application to a flow-through reactor. *Journal of Bioscience and Bioengineering*, *105*, 687–689.

Sanpo, N., Ang, S. M., Cheang, P., & Khor, K. A. (2009). Antibacterial property of cold sprayed chitosan–Cu/Al coating. *Journal of Thermal Spray Technology*, *18*, 600–608.

Spasova, M., Paneva, D., Manolova, N., Radenkov, P., & Rashkov, I. (2008). Electrospun chitosan-coated fibers of poly(L-lactide) and poly(L-lactide)/poly(ethylene glycol): Preparation and characterization. *Macromolecular Bioscience*, *8*, 153–162.

Su, D. S. (2009). The use of natural materials in nanocarbon synthesis. *Chemsuschem*, *2*, 1009–1020.

Wang, X. Y., Du, Y. M., & Luo, J. W. (2008). Biopolymer/montmorillonite nanocomposite: Preparation, drug-controlled release property and cytotoxicity. *Nanotechnology*, *19*, 065707.

Wang, X. Y., Pei, X. F., Du, Y. M., & Li, Y. (2008). Quaternized chitosan/rectorite intercalative materials for a gene delivery system. *Nanotechnology*, *19*, 375102.

Wang, X. Y., Du, Y. M., Sun, R. C., & Liu, C. F. (2009). Antimicrobial activity of quaternized chitosan/organic rectorite nanocomposite. *Journal of Inorganic Materials*, *24*, 1236–1242.

Wang, X. Y., Du, Y. M., Luo, J. W., Lin, B. F., & Kennedy, J. F. (2007). Chitosan/organic rectorite nanocomposite films: Structure, characteristic and drug delivery behaviour. *Carbohydrate Polymers*, *69*, 41–49.

Wang, X. Y., Du, Y. M., Yang, H. H., Wang, X. H., Shi, X. W., & Hu, Y. (2006). Preparation, characterization and antimicrobial activity of chitosan/layered silicate nanocomposites. *Polymer*, *47*, 6738–6744.

Wang, X. Y., Du, Y. M., Luo, J. W., Yang, J. H., Wang, W. P., & Kennedy, J. F. (2009). A novel biopolymer/rectorite nanocomposite with antimicrobial activity. *Carbohydrate Polymers*, *77*, 449–456.

Wu, J., Wei, W., Wang, L. Y., Su, Z. G., & Ma, G. H. (2007). A thermosensitive hydrogel based on quaternized chitosan and poly(ethylene glycol) for nasal drug delivery system. *Biomaterials*, *28*, 2220–2232.

Wypych, F., & Satyanarayana, K. G. (2005). Functionalization of single layers and nanofibers: A new strategy to produce polymer nanocomposites with optimized properties. *Journal of Colloid and Interface Science*, *285*, 532–543.

Yang, A., Tao, X. M., Pang, G. K. H., & Siu, K. G. G. (2008). Preparation of porous tin oxide nanobelts using the electrospinning technique. *Journal of the American Ceramic Society*, *91*, 257–262.

Yu, D. G., Shen, X. X., Branford-White, C., White, K., Zhu, L. M., & Bligh, S. W. A. (2009). Oral fast-dissolving drug delivery membranes prepared from electrospun polyvinylpyrrolidone ultrafine fibers. *Nanotechnology*, *20*, 055104.

Zhang, Y. Y., Huang, X. B., Duan, B., Wu, L. L., Li, S., & Yuan, X. Y. (2007). Preparation of electrospun chitosan/poly(vinyl alcohol) membranes. *Colloid and Polymer Science*, *285*, 855–863.

Zhou, Y. S., Yang, D. Z., & Nie, J. (2007). Effect of PVA content on morphology, swelling and mechanical property of crosslinked chitosan/PVA nanofibre. *Plastics Rubber and Composites*, *36*, 254–258.

Zhu, A. P., Chen, T., Yuan, L. H., Wu, H., & Lu, P. (2006). Synthesis and characterization of N-succinyl-chitosan and its self-assembly of nanospheres. *Carbohydrate Polymers*, *66*, 274–279.